Journal of Magnetism and Magnetic Materials 456 (2018) 439–443

Contents lists available at ScienceDirect

Journal of Magnetism and Magnetic Materials

journal homepage: www.elsevier.com/locate/jmmm

Research articles

Magnetocaloric effect and its modulation by electric field in $La_{0.325}Pr_{0.3}Ca_{0.375}MnO_3$ films grown on (0 1 1)-PMN-PT substrates

K.M. Qiao [a,b], J. Li [a,b], Y. Liu [a,b], H. Kuang [a,b], J. Wang [a,b,*], F.X. Hu [a,b,*], J.R. Sun [a,b], B.G. Shen [a,b]

[a] Beijing National Laboratory for Condensed Matter Physics & State Key Laboratory of Magnetism, Institute of Physics, Chinese Academy of Sciences, Beijing 100190, PR China
[b] School of Physical Sciences, University of Chinese Academy of Sciences, Beijing 100049, PR China

ARTICLE INFO

Article history:
Received 29 September 2017
Received in revised form 8 December 2017
Accepted 23 January 2018
Available online 3 February 2018

ABSTRACT

In this paper, we have investigated the magnetocaloric effect (MCE) and its modulation by electric field in $La_{0.325}Pr_{0.3}Ca_{0.375}MnO_3$ (LPCMO) films grown on (0 1 1)-oriented PMN-PT substrates. As a typical perovskite manganite with phase separation, the LPCMO bulk shows a considerable MCE, but the MCE of the LPCMO films has never been investigated. We found that the LPCMO films exhibit a MCE over a wide temperature range. A modulation of magnetization by electric field has been observed in the temperature dependent (M–T) and magnetic field dependent (M–H) curves. As a result, enhanced magnetic entropy change and refrigeration capacity by about 4% under an electric field of +6 kV/cm has been demonstrated.

1. Introduction

Magnetic refrigeration is regarded as an environmentally friendly and energy saving refrigeration technique for substituting the conventional vapor compression refrigeration. To develop appropriate materials as magnetic refrigerants has been a long-term concern. The push for energy-efficient magnetic refrigeration based on magnetocaloric effect (MCE) has attracted much interest in recent years, fueling much more researches into magnetocaloric materials, such as complex oxides [1]. The strongly correlated manganite $R_{1-x}M_xMnO_3$ (R = La, Pr, Nd, Sm and M = Sr, Ca, Ba, Pb) show a variety of interesting magnetic and transport phenomena [2–4] due to the strong interactions among lattice, charge, spin and orbital degrees of freedom [5]. $La_{0.325}Pr_{0.3}Ca_{0.375}MnO_3$ is a typical strong correlated manganite, where phase separation between an insulation antiferromagnetic charge-ordered (CO) phase and a metallic ferromagnetic (FM) phase has been previously demonstrated [6–8]. Charge ordering refers to the periodic arrangement of Mn^{3+} and Mn^{4+} cations within a crystal lattice, which is a common phenomenon in the narrow bandwidth manganites [9,10]. Materials with such phase-separation usually exhibit high sensitivity to external parameters, such as magnetic field, electric field, strain, doping, pressure, and light illumination [11–16], resulting in fascinating multifunctional properties. An introduced strain by electric field, for the film grown on a relaxor ferroelectric substrate, largely impacts the interactions, thus novel magnetic and electric properties have been observed, such as the preferential formation of elongated ferromagnetic clusters [5,17], and anisotropic magnetic memory effect [17,18]. Once applying an electric field on the ferroelectric substrate, a strain can be generated and then transferred to the film grown on it, leading to a change in the magnetic properties. This is one phenomenon of the so-called magnetoelectric coupling (ME). ME effect has been under intensive study for various potential applications. A common method to attain the ME coupling is using the artificial ferromagnetic (ferrimagnetic)/piezoelectric bilayer structures [19], in which excellent ME performance can be realized via strain-mediated mechanism. Recently, the electric field control of magnetic anisotropy, saturation magnetization, memory effect [17,18], exchange bias, magnetization reversal, and magnetocaloric effect have been experimentally demonstrated in various artificial systems. Moya et al. reported giant MCE in $La_{0.7}Ca_{0.3}MnO_3$ epitaxial films using strain-mediated feedback from $BaTiO_3$ substrates due to structural phase transition [20]. Gong et al. studied the strain-mediated ME effect in the NiMnIn ribbons pasted on PMN-PT substrate [19] and observed tunable MCE in the bilayers of $FeRh_{0.96}Pd_{0.04}$/PMN-PT [21] by electric field.

For the typical manganite perovskites $La_{0.35}Pr_{0.275}Ca_{0.375}MnO_3$ (LPCMO) with phase separation, Phan et al. have investigated the MCE in the bulk and nanocrystalline particles [2], but the MCE of the LPCMO films have never been investigated. Here, we report the magnetic and magnetocaloric properties and their modulation of by electric field in LPCMO films grown on the relaxor ferroelectric substrates of (0 1 1)-0.7Pb($Mg_{1/3}Nb_{2/3}$)O_3-0.3$PbTiO_3$(PMN-PT).

* Corresponding authors at: Beijing National Laboratory for Condensed Matter Physics & State Key Laboratory of Magnetism, Institute of Physics, Chinese Academy of Sciences, Beijing 100190, PR China.
E-mail addresses: fxhu@iphy.ac.cn (F.X. Hu), wangjing@iphy.ac.cn (J. Wang).

https://doi.org/10.1016/j.jmmm.2018.01.067
0304-8853/

2. Experiments

LPCMO thin film was deposited on (0 1 1)-oriented PMN-PT single crystal substrate using pulsed laser deposition (PLD) technique. The LPCMO target was prepared by conventional solid reaction methods. We used the commercial (0 1 1)-oriented PMN-PT single crystal substrate because of its excellent converse piezoelectric effect and perovskite cubic structure (a_{PMN-PT} = 4.017 Å). The temperature of the substrate was kept at 670 °C and the oxygen pressure at 100 Pa during the deposition process. After deposition, the film was cooled down to room temperature in 1 atm oxygen atmosphere. The film thickness is about 200 nm, which was determined by X-ray reflectivity measurements. The crystalline structure and orientation of the film were determined by means of X-ray diffraction (XRD) using Cu-Kα radiation (see Fig. 1). Au layers were vapor deposited on bottom side of LPCMO/PMN-PT heterostructure as electrodes. The magnetic properties of the samples were measured using a superconducting quantum interference device (SQUID-VSM) with in situ electric fields applied across the LPCMO/PMN-PT structure (along the out plane [0 1 1] direction) by a Keithley 6517B electrometer. The leakage current is below 5 nA under a 6 kV/cm electric field. The PMN-PT substrates have not specially poled but four cycles up to ± 6 kV/cm were performed prior to the measurements.

3. Results and discussions

XRD measurements indicate that the LPCMO bulk crystallizes in orthorhombic structure with space group of Pnma and the pseudocubic lattice parameters are determined to be 3.823 Å (a = 5.430 Å, b = 7.658 Å, and c = 5.433 Å). The XRD patterns indicate the oriented growth of LPCMO films along [1 1 0] direction, as shown in Fig. 1.

To explore the impact of strain-mediated magnetic properties in the LPCMO/PMN-PT heterostructure, temperature dependent magnetization (M–T) along the in-plane [01–1] direction was measured, as shown in Fig. 2(a). The measurements of M–T curves were firstly performed in the cooling process from 300 K to 10 K and followed by warming from 10 K to 300 K under a magnetic field of 0.01 T along in-plane [01–1] direction (black curves in Fig. 2(a)). Then, at 300 K, a + 6 kV/cm electric field was applied, and the next M–T curves were measured on cooling and warming under the applications of both a + 6 kV/cm electric field and a 0.01 T magnetic field (red curves in Fig. 2(a)). From Fig. 2(a), one can notice the large modulation of magnetization by the electric field. During the measurements, the sweep rate of temperature is 5 K/min.

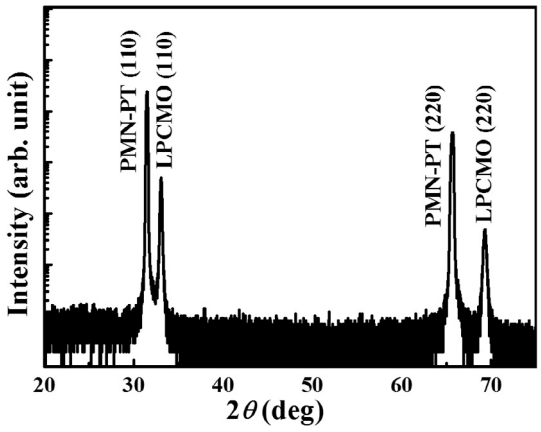

Fig. 1. X-ray diffraction patterns of the LPCMO/PMN-PT heterostructure, where logarithmic y-axis is adopted.

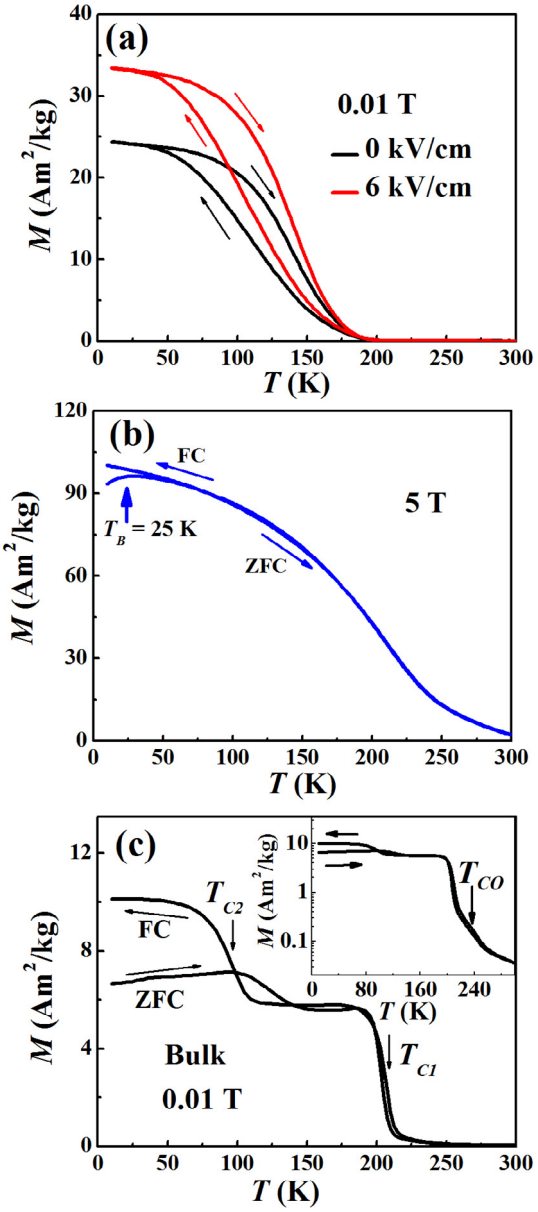

Fig. 2. (a) Temperature dependent magnetization (M–T) for LPCMO film under 0.01 T with and without application of +6 kV/cm for the magnetic field along in-plane [01–1] direction. (b) The ZFC-FC magnetization under 5 T on warming and cooling. (c) The M–T curves under 0.01 T for LPCMO bulk measured using ZFC-FC modes, where the inset shows the M–T with a logarithmic scale adopted in y-axis. The arrows indicate the directions of sweeping temperature.

For comparison, we also measured the M–T curves of the bulk under a magnetic field of 0.01 T in the absence of electric field using ZFC (zero field cooling) – FC (field cooling) modes, as shown in Fig. 2(c). Clearly, the bulk sample undergoes successive multiple magnetic transitions, consistent with the previously reported [22]. Here, the magnetic transition T_{C1} or T_{C2} is defined as the temperature where the minimum of the dM/dT occurs. The CO transition T_{CO} can only be identified in the M–T curve where a logarithmic scale is adopted in y-axis (inset of Fig. 2(c)), which is defined as the temperature where the largest change occurs in the slope. The T_{CO} first occurs at round 225 K (inset of Fig. 2(c)), and then a steep increase in magnetization at around $T_{C1} \sim 210$ K appears, which comes from the development of FM clusters within the background of CO state [22]. As temperature is further decreased, the magnetization increases again at around $T_{C2} \sim 100$ K, which

is caused by the growth of the FM clusters. For the temperature from T_{C1} down to T_{C2}, the fraction of the frozen isolated FM clusters keeps nearly unchanged in the background of CO state. With the further decrease of temperature, the magnetization exhibits a plateau below 75 K again, which indicates that the FM clusters have no further evolution and the FM volume fraction also becomes constant [22]. The different magnetization at low temperature in the heating (ZFC mode) and cooling branch (FC mode) for the bulk originates from the coexistence of FM and CO clusters and the possible pinning effect of CO-AFM on FM domains.

However, the case is very different for the LPCMO film, which only undergoes a paramagnetic to ferromagnetic (FM) transition at around 200 K (Fig. 2(a)). No clear CO transition can be identified in the film. This indicates that the CO state is suppressed to a great extent and the FM order is established in the background of CO state for the film [8]. Besides, the $M-T$ curves of LPCMO films show a bulk-like hysteresis, which is common and originates from the existence of separated FM and CO phases. On cooling, FM phase is gradually developed from the background of CO phase. While on the warming process, the FM phase is frozen, leading to an increased magnetic moment relative to the cooling process [23]. Interestingly, with the application of electric field, the magnetization under a small magnetic field of 0.01 T increases when the temperature is below the FM transition temperature (200 K) (Fig. 2(a)). The relative change, defined as $\Delta M/M(0) = (M(E) - M(0))/M(0)$, is up to 37% at 10 K when an electric field of + 6 kV/cm is applied, where $M(E)$ and $M(0)$ correspond to the magnetizations with and without the electric field, respectively. This result indicates an obvious ME effect under a small magnetic field of 0.01 T. However, the ME effect, i.e. ΔM, becomes weak with increasing temperature and vanishes at the temperature above the FM transition point, as shown in Fig. 2(a). The electric-field control of magnetization in LPCMO/PMN-PT should originate from the modulation of electric-field on the phase separation, as discussed previously [5,17,24]. Actually, the cooling curves measured after removing the electric field are the same as the curves measured in a normal magnetic-field-cooling process because the magnetic state at 300 K become paramagnetic, which indicates that the ME effect is completely reversible. In addition, the $M-T$ curves were also measured using ZFC-FC modes at a 5 T magnetic field on warming and cooling in the absence of electric field, as shown in Fig. 2(b). One can notice that a clear bulge of magnetization around $T_B \sim 25$ K appears in the warming branch (ZFC mode), which might be relative to the possible unblocking of the low temperature frozen charge ordering-antiferromagnetic (CO-AFM) state [8]. The LPCMO film is blocked in a metastable state dominated by the CO-AFM state at low temperatures. With the temperature increasing with an applied magnetic field, the system was unblocked, which promotes a growth of the FM phase over the CO-AFM one. Such a behavior predicts that an inverse MCE may occur at temperatures below 25 K. For the cooling branch, the anomaly of magnetization around 25 K and the thermal hysteresis disappears. This result indicates that the frozen CO state may have been converted into FM on cooling with a high magnetic field of 5 T applied.

To study the magnetocaloric property and its modulation by electric field in LPCMO films, we measured the isothermal magnetization ($M-H$) curves on warming for the LPCMO/PMN-PT heterostructures at different temperatures with and without electric field, as shown in Fig. 3(a)–(c). The sweep rate of magnetic field is 100 Oe/s within 0–1 T and 500 Oe/s within 1–5 T. The magnetic

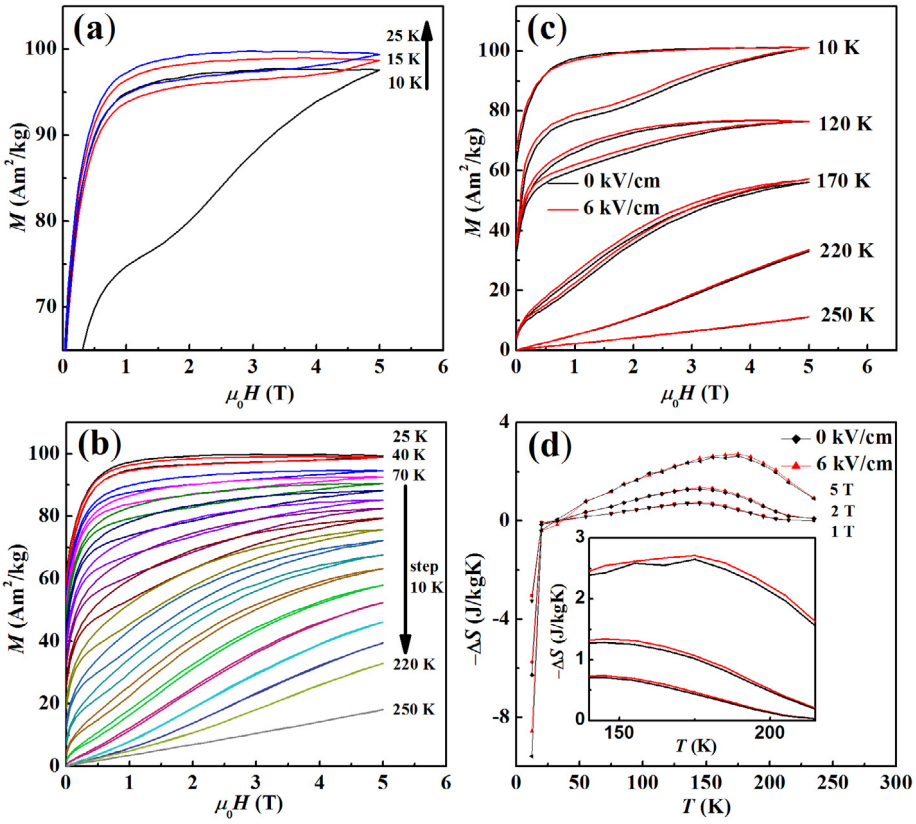

Fig. 3. The isothermal magnetization ($M-H$) curves for LPCMO/PMN-PT heterostructures measured in the absence of electric field at different temperatures (a) 10 K, 15 K, and 25 K and (b) from 25 K to 250 K, where the arrows indicate the temperature warming direction. (c) The comparison of $M-H$ curves with and without + 6 kV/cm for some representative temperatures. (d) The comparison of magnetic entropy change ΔS with and without + 6 kV/cm under different magnetic fields, where the inset shows the details of the ΔS comparison.

field was applied along in-plane [01–1] direction while the electric field along the out plane [0 1 1] direction. The sample was first cooled down to 10 K with an applied electric field of + 6 kV/cm and then the measurements of isothermal $M–H$ curves were performed on warming from 10 K to 250 K without changing the electric field. After the measurements, the sample was heating to 300 K and removed the electric field. Then, the sample was similarly re-cooled down to 10 K and the isothermal $M–H$ curves were measured on warming without applying the electric field. One can notice that the film exhibits obvious field hysteresis losses below the FM transition temperature, which become more prominent with temperature decreasing. This is caused by the coexistence of CO-AFM and FM phases below the transition temperature and the development of the FM phase with temperature decreasing. Moreover, in accordance with the $M–T$ curve measured at 5 T on heating (inset of Fig. 2(a)), the magnetization anomaly around 25 K is also demonstrated during the measurements of $M–H$ curves. The saturated magnetization first increases as the temperature increases from 10 K to 25 K (Fig. 3(a)). Then the saturated magnetization normally deceases with further increasing the temperature from 25 K to 250 K, which is the typical FM character (Fig. 3(b)). Such a behavior will lead to an appearance of inverse MCE below 25 K and a normal MCE above 25 K, as shown in Fig. 3(c).

For some complex magnetic systems with hysteretic behavior, an insufficient measurement protocol sometimes can lead to a false value of entropy change ΔS [25,26].We also measured the isothermal magnetization ($M–H$ curves) in the loop mode [25,26] on both heating and cooling process, and found that the obtained $M–H$ curves accord with the ones measured on heating in normal mode at temperatures well above $T_B \sim 25$ K, noting that the thermal hysteresis nearly disappears in the $M–T$ curve as a high magnetic field of 5 T was applied (Fig. 2(b)). This result indicates that the evaluated ΔS values measured in normal mode on heating are reliable for the present films.

The shape of $M–H$ curves measured under applying an electric field of + 6 kV/cm is very similar to the ones in the absence of electric field except some enhancements of the magnetization. Fig. 3(c) presents the comparison of $M–H$ curves with and without electric field for some representative temperatures. At every temperature below the FM transition, the application of + 6 kV/cm can lead to an enhanced magnetization in the almost entire $M–H$ curves, particularly for the branch of H increasing. But the enhancement is getting smaller with increasing temperature and vanishes at paramagnetic state. As an electric field of + 6 kV/cm was applied along the out-plane [0 1 1] direction of PMN-PT substrate, the in-plane [01–1] direction undergoes a tensile strain [17], which should be responsible for the enhancement of the magnetization in the $M–H$ curves. Previous studies [5,17] have demonstrated that a tensile strain can lead to a preferential formation of elongated FM domains for a manganite with phase separation. In other words, the FM domains prefer to grow along a tensile strain direction during the formation of magnetic ordering in the cooling process from the paramagnetic state [5,17,18]. A tensile strain bends the Mn-O-Mn bonds and may cause a strong overlap of the electronic clouds, hence strengthen the FM exchange interaction and result in an enhancement of magnetization.

Based on the isothermal $M–H$ results, magnetic entropy change ΔS with and without electric field is calculated by Maxwell relation, as shown in Fig. 3(d). The mass of LPCMO film (200 nm) was evaluated by using a density of 5.978 g cm^{-3}, which is estimated based on the structure and lattice parameters of LPCMO. An inverse ΔS appears below 25 K as expected due to the possible frozen of long-range FM and CO phases below T_B. The ΔS value at 10 K is about 11.4 J/kgK and 10.2 J/kgK for the cases with and without + 6 kV/cm. The enhancement ratio by electric field is about 11.8%. At temperatures above 25 K, the film displays normal ΔS in a very wide temperature range due to the sizable window of the FM transition. The maximal value of $-\Delta S$ is about 3.1 J/kgK and 2.9 J/kgK around 175 K under a magnetic change of 0–5 T for the cases with and without + 6 kV/cm, respectively, and the half width of ΔS peak is about 145 K. In particular, the $-\Delta S$ (about 1.3 J/kgK) under 2 T (permanent magnet can reach) is comparable to that of well-known metamagnetic Ni-Co-Mn-In film (1.1 J/kgK, 2 T) [27] and Ni-Mn-In-Cr film (1.3 J/kgK, 2 T) [28], but somewhat smaller than that of Ni-Mn-In thin film (2 J/kgK, 2 T) [29] and Ni-Mn-Ga-Co film (3.5 J/kgK, 2 T) [30]. One knows that the refrigerant capacity (RC) is also a parameter to evaluate the MCE of a material. RC is a measure of energy that the MCE material can transfer between hot and cold sources, which is defined as $RC = \int_{T_2}^{T_1} |\Delta S(T)|_{\Delta H} dT$, where T_1 and T_2 refer to the temperatures corresponding to the full width at half maximum in the $|\Delta S_M(T)|$ curves. The RC values estimated for the film under a magnetic field change of 0–2 T is about 70.4 J/kg, which is larger than that of the reported Ni-Mn-Sn thin films (RC $\sim$ 33.9 J/kg for 0–2 T) [31]. The evaluated RC of 0–5 T in the present film is about 443 J/kg and 425 J/kg for the cases with and without +6 kV/cm, respectively. The enhancement ratio of $-\Delta S$ and the RC by electric field is about 4% around 175 K. All the results have demonstrated the fact that the enhancement of the MCE by electric field via strain-mediated ME coupling.

4. Conclusions

In summary, we have studied magnetocaloric effect and its modulation by electric field in LPCMO/PMN-PT heterostructure. The LPCMO film shows an inverse entropy change ΔS with a maximal value of 11.4 J/kgK below 25 K. The reason can be ascribed to the possible frozen of long-range FM and CO phases. Meanwhile, normal ΔS appears in a wide temperature above 25 K. The maximal $-\Delta S$ value is about 2.9 J/kgK around 175 K and RC $\sim$ 425 J/kg for a magnetic change of 0–5 T. An application of electric field + 6 kV/cm along the out-plane [0 1 1] direction of PMN-PT substrate causes a tensile strain along in-plane [01–1] direction, which increases the magnetization due to ME effect, and hence leads to an enhancement of $-\Delta S$ and RC by 4%. The modulation of magnetocaloric effect by electric field is of particular significance for exploring multifield driven refrigeration technique.

Acknowledgements

This work was supported by the National Key Research and Development Program of China (Grant No. 2017YFB0702702, 2014CB643700, 2017YFA0303601 and 2016YFB0700903), the National Natural Sciences Foundation of China (Grant No. 51531008, 51771223, 51590880, 11674378 and 11474341), the Key Program and Strategic Priority Research Program (B) of the Chinese Academy of Sciences.

References

[1] M.H. Phan, S.C. Yu, J. Magn. Magn. Mater. 308 (2007) 325.
[2] M.H. Phan, S. Chandra, N.S. Bingham, H. Srikanth, C.L. Zhang, S.W. Cheong, T.D. Hoang, H.D. Chinh, Appl. Phys. Lett. 97 (2010) 242506.
[3] Y. Tokura, Y. Tomioka, J. Magn. Magn. Mater. 200 (1999) 1.
[4] M. Michelmann, V. Moshnyaga, K. Samwer, Phys. Rev. B. 85 (2012) 014424.
[5] T.Z. Ward, J.D. Budai, Z. Gai, J.Z. Tischler, Lifeng Yin, J. Shen, Nat. Phys. 5 (2009) 885.
[6] Z.B. Guo, Y.W. Du, J.S. Zhu, H. Huang, W.P. Ding, D. Feng, Phys. Rev. Lett. 78 (1997) 1142.
[7] L. Ghivelder, F. Parisi, Phys. Rev. B. 71 (2005) 184425.
[8] M.H. Phan, M.B. Morales, N.S. Bingham, H. Srikanth, Phys. Rev. B. 81 (2010) 094413.
[9] Y. Tomioka, A. Asamitsu, Y. Moritomo, H. Kuwahara, Y. Tokura, Phys. Rev. Lett. 74 (1995) 5108.

[10] N.S. Bingham, P. Lampen, M.H. Phan, H. Srikanth, Phys. Rev. B. 86 (2012) 064420.
[11] T. Wu, S.B. Ogale, S.R. Shinde, Amlan Biswas, T. Polletto, R.L. Greene, T. Venkatesan, A.J. Millis, J. Appl. Phys. 93 (2003) 5507.
[12] Y. Tomioka, A. Asamitsu, H. Kuwahara, Y. Moritomo, Y. Tokura, Phys. Rev. B. 53 (1996) 1689.
[13] K. Miyano, T. Tanaka, Y. Tomioka, Y. Tokura, Phys. Rev. Lett. 78 (1997) 4257.
[14] M. Fiebig, K. Miyano, Y. Tomioka, Y. Tokura, Science 280 (1998) 5371.
[15] V. Kiryukhin, B.G. Kim, V. Podzorov, S.-W. Cheong, T.Y. Koo, J.P. Hill, I. Moon, Y. H. Jeong, Phys. Rev. B. 63 (2000) 024420.
[16] J. Wang, F.X. Hu, R.W. Li, J.R. Sun, B.G. Shen, Appl. Phys. Lett. 96 (2010) 052501.
[17] Y.Y. Zhao, J. Wang, H. Kuang, F.X. Hu, H.R. Zhang, Y. Liu, Y. Zhang, S.H. Wang, R. R. Wu, M. Zhang, L.F. Bao, J.R. Sun, B.G. Shen, Sci. Rep. 4 (2014) 7075.
[18] Y.Y. Zhao, J. Wang, H. Kuang, F.X. Hu, Y. Liu, R.R. Wu, X.X. Zhang, J.R. Sun, B.G. Shen, Sci. Rep. 5 (2015) 9668.
[19] Y.Y. Gong, D.H. Wang, Q.Q. Cao, E.K. Liu, J. Liu, Y.W. Du, Adv. Mater. 27 (2015) 801.
[20] X. Moya, F. Maccherozzi, A.I. Tovstolytkin, N.D. Mathur, Nat. Mater. 12 (2012) 3463.
[21] Q.B. Hu, J. Li, C.C. Wang, Z.J. Zhou, Q.Q. Cao, T.J. Zhou, D.H. Wang, Y.W. Du, Appl. Phys. Lett. 110 (2017) 222408.
[22] P. Levy, F. Parisi, M. Quintero, L. Granja, J. Curiale, J. Sacanell, G. Leyva, G. Polla, Phys. Rev. B. 65 (2002) 140401.
[23] D. Gillaspie, J.X. Ma, H.Y. Zhai, T.Z. Ward, H.M. Christen, E.W. Plummer, J. Shen, J. Appl. Phys. 99 (2006) 08S901.
[24] Q.P. Chen, J.J. Yang, Y.G. Zhao, S. Zhang, J.W. Wang, M.H. Zhu, Y. Yu, X.Z. Zhang, Zhu Wang, Bin Yang, D. Xie, T.L. Ren, Appl. Phys. Lett. 98 (2011) 172507.
[25] R. Niemann, O. Heczko, L. Schultz, S. Fähler, Int. J. Refrig. 37 (2014) 281.
[26] L. Caron, N.B. Doan, L. Ranno, J. Phys.: Condens. Matter. 29 (2017) 075401.
[27] R. Niemann, O. Heczko, L. Schultz, S. Fähler, Appl. Phys. Lett. 97 (2010) 222507.
[28] H.S. Akkera, I. Singh, D. Kaur, J. Magn. Magn. Mater. 424 (2017) 194.
[29] H.S. Akkera, I. Singh, D. Kaur, J. Alloy. Compd. 642 (2015) 53.
[30] B. Schleicher, R. Niemann, S. Schwabe, R. Hühne, L. Schultz, K. Nielsch, S. Fähler, Sci. Rep. 7 (2017) 14462.
[31] E. Yuzuak, I. Dincer, Y. Elerman, A. Auge, N. Teichert, A. Hutten, Appl. Phys. Lett. 103 (2013) 222403.